Environ. Sci. Technol. **2009,** *43,* 7416–7422

Thermodynamic Properties of Autunite, Uranyl Hydrogen Phosphate, and Uranyl Orthophosphate from Solubility and Calorimetric Measurements

DREW GORMAN-LEWIS,*,† TATIANA SHVAREVA,‡ KARRIE-ANN KUBATKO,†,# PETER C. BURNS,† DAWN M. WELLMAN,§ BRUCE MCNAMARA,§ JENNIFER E. S. SZYMANOWSKI,† ALEXANDRA NAVROTSKY,‡ AND JEREMY B. FEIN†

Department of Civil Engineering and Geological Sciences, University of Notre Dame, 156 Fitzpatrick Hall, Notre Dame, Indiana 46556, Peter A. Rock Thermochemistry Laboratory, University of California Davis, One Shields Avenue, Davis, California 95616, and Pacific Northwest National Laboratory, P.O. Box 999, Richland, Washington 99352

Received May 4, 2009. Revised manuscript received August 11, 2009. Accepted August 13, 2009.

In this study, we use solubility and drop-solution calorimetry measurements to determine the thermodynamic properties of the uranyl phosphate phases autunite, uranyl hydrogen phosphate, and uranyl orthophosphate. Conducting the solubility measurements from both supersaturated and undersaturated conditions and under different pH conditions rigorously demonstrates attainment of equilibrium and yields well-constrained solubility product values. We use the solubility data and the calorimetry data, respectively, to calculate standard-state Gibbs free energies of formation and standard-state enthalpies of formation for these uranyl phosphate phases. Combining these results allows us also to calculate the standard-state entropy of formation for each mineral phase. The results from this study are part of a combined effort to develop reliable and internally consistent thermodynamic data for environmentally relevant uranyl minerals. Data such as these are required to optimize and quantitatively assess the effect of phosphate amendment remediation technologies for uranium contaminated systems.

Introduction

Uranium is a prominent contaminant in a number of groundwater aquifer settings. Its presence in these systems in soluble form is of concern due to its chemical toxicity and potential radiological exposure hazard. Subsurface polyphosphate application represents a promising remediation technology for uranium contamination of groundwater aquifers. In this approach, focused application of polyphosphate can reduce the concentration of aqueous uranium through direct precipitation of uranyl phosphate minerals (*1*). Modeling and optimization of this approach requires knowledge of thermodynamic properties for the range of uranyl phosphate mineral phases that can form under realistic environmental conditions. Although the thermodynamic properties of some environmentally relevant uranyl phosphate phases have been measured (e.g., see ref *2* for a recent review of the available solubility data), the data set lacks some crucial phases, and the thermodynamic properties for some of the uranyl phosphate phases that have been studied are poorly constrained.

In this study, we measured the solubilities of uranyl hydrogen phosphate ($UO_2HPO_4 \cdot 3H_2O$) (abbreviated as HUP), uranyl orthophosphate ($(UO_2)_3(PO_4)_2 \cdot 4H_2O$) (UP), and autunite ($Ca[(UO_2)(PO_4)]_2 \cdot 3H_2O$) (CaUP), using the results to determine the Gibbs free energies of formation of each phase. In addition, we used high-temperature oxide melt solution calorimetry to yield the enthalpies of formation of HUP and UP. The Gibbs free energies and enthalpies of formation were also used to calculate the entropy of formation and standard entropy for HUP and UP phases. These thermodynamic parameters not only enable the determination of the relative stabilities of these environmentally relevant uranyl phosphate phases as a function of fluid composition, but also enable calculation of the effects of polyphosphate amendment on the extent of uranium removal in geologic systems where uranium mobility is primarily controlled by one of these three phases.

Experimental Section

Syntheses of Solid Phases. ACS grade reagents and 18 MΩcm H_2O were used in all syntheses. Teflon-lined Parr bombs were used for the hydrothermal treatments of the starting material. HUP was prepared by adding 0.14 g of Na_2HPO_4, 0.42 g of $UO_2(CH_3COO)_2(H_2O)_2$, and 5 cm^3 of H_2O to a Teflon lined Parr bomb and heating for 7 d at 150 °C. UP was synthesized by adding 0.14 g of Na_2HPO_4, 2 cm^3 of 0.50 M $UO_2(NO_3)_2$, and 3 cm^3 of H_2O to a Teflon lined Parr bomb and heating for 7 d at 150 °C. After synthesis, all batches of minerals were rinsed 3 times with 25 cm^3 aliquots of boiling H_2O and air-dried prior to characterization (additional syntheses details and results of characterization are found in the Supporting Information).

The CaUP used was a natural sample, described by Wellman et al. (*1*) to be 98−99% pure hydrous CaUP with a stoichiometry of $Ca(UO_2)_2(PO_4)_2 \cdot 3H_2O$.

Solubility Experiments. All solubility measurements were conducted as batch experiments at ca. 25 °C using Teflon reaction vessels. An Orion combination pH electrode that was calibrated daily with 4 NIST standards (pH 2, 4, 7, and 10) was used for pH measurements. The ionic strength of the buffers was not perfectly matched to the ionic strength of the experiments; however, the additional error associated with pH measurements as a result of the difference in ionic strength and residual liquid-junction potential error is likely much smaller than experimental error which dominates the stated uncertainties for the calculated thermodynamic parameters (*3*). Two types of experiments were performed: undersaturated experiments were conducted by adding ∼350 mg of the solid phase of interest to ∼125 cm^3 of H_2O; supersaturated experiments involved adding ∼350 mg of the mineral phase to aqueous

* Corresponding author present address: University of Washington, Department of Earth and Space Sciences, 070 Johnson Hall, Seattle, WA 98195; phone: 206-543-3541; fax: 206-543-0489; e-mail: dgormanl@u.washington.edu.
† University of Notre Dame.
‡ University of California Davis.
§ Pacific Northwest National Laboratory.
# Current address: The Ohio State University, Civil & Environmental Engineering & Geodetic Science, Columbus, OH 43210.

10.1021/es9012933 CCC: $40.75
Published on Web 09/03/2009

TABLE 1. Thermodynamic Cycles for the Calculation of Enthalpies of Formation of HUP and UP from Oxides and Elements[a]

$UO_2HPO_4 \cdot 3H_2O$, uranyl hydrogen phosphate (HUP)	
$UO_2HPO_4 \cdot 3H_2O_{xl,25\ °C} = UO_{3\ sln,702\ °C} + 0.5\ P_2O_{5\ sln,702\ °C} + (3 + 0.5)\ H_2O_{g,702\ °C}$	$\Delta H1 = \Delta H_{ds}(HUP) = 411.02 \pm 3.46$ kJ/mol (7 drops)[b]
$UO_{3xl,25\ °C} = UO_{3\ sln,702\ °C}$	$\Delta H2 = \Delta H_{ds}(UO_3)$ (*10*)
$P_2O_{5xl,25\ °C} = P_2O_{5sln,702\ °C}$	$\Delta H3 = \Delta H_{ds}(P_2O_5)$ (*11*)
$H_2O_{l,25\ °C} = H_2O_{g,702\ °C}$	$\Delta H4 = \Delta H_{ds}(H_2O)$ (*12*)
$UO_{3xl,25\ °C} + 0.5P_2O_{5xl,25\ °C} + (3 + 0.5)\ H_2O_{l,25\ °C} = UO_2HPO_4 \cdot 3H_2O_{xl,25\ °C}$	$\Delta H5 = \Delta H_{f,ox}(HUP) = -\Delta H1 + \Delta H2 + 0.5\ \Delta H3 + 3.5\ \Delta H4 = -240.95 \pm 3.89$ kJ/mol
$U_{xl,25\ °C} + 3/2O_{2g,25\ °C} = UO_{3xl,25\ °C}$	$\Delta H6 = \Delta H_f\ UO_3$ (*12*)
$2P_{xl,25\ °C} + 5/2O_{2g,25\ °C} = P_2O_{5xl,25\ °C}$	$\Delta H7 = \Delta H_f\ P_2O_5$ (*12*)
$H_{2g,25\ °C} + 1/2O_{2g,25\ °C} = H_2O_{l,25\ °C}$	$\Delta H8 = \Delta H_f\ H_2O$ (*12*)
$U_{xl,25\ °C} + P_{xl,25\ °C} + 7/2\ H_{2g,25\ °C} + 9/2O_{2g,\ 25\ °C} = UO_2HPO_4 \cdot 3H_2O_{xl,25\ °C}$	$\Delta H9 = \Delta H_{f,el}(HUP) = \Delta H5 + \Delta H6 + 0.5\ \Delta H7 + 3.5\ \Delta H8 = -3223.22 \pm 3.99$ kJ/mol
$(UO_2)_3(PO_4)_2 \cdot 4H_2O$, uranyl orthophosphate (UP)	
$(UO_2)_3(PO_4)_2 \cdot 4H_2O_{xl,25\ °C} = 3UO_{3sln,702\ °C} + P_2O_{5sln,702\ °C} + 4H_2O_{g,702\ °C}$	$\Delta H10 = \Delta H_{ds}(UP) = 821.38 \pm 13.71$ kJ/mol (8 drops)[b]
$UO_{3xl,25\ °C} = UO_{3sln,702\ °C}$	$\Delta H2 = \Delta H_{ds}(UO_3)$ (*10*)
$P_2O_{5xl,25\ °C} = P_2O_{5sln,702\ °C}$	$\Delta H3 = \Delta H_{ds}(P_2O_5)$ (*11*)
$H_2O_{l,25\ °C} = H_2O_{g,702\ °C}$	$\Delta H4 = \Delta H_{ds}(H_2O)$ (*12*)
$3UO_{3xl,25\ °C} + P_2O_{5xl,25\ °C} + 4\ H_2O_{l,25\ °C} = (UO_2)_3(PO_4)_2 \cdot 4H_2O_{xl,25\ °C}$	$\Delta H11 = \Delta H_{f,ox}(UP) = -\Delta H10 + 3\Delta H2 + \Delta H3 + 4\Delta H4 = -681.51 \pm 13.82$ kJ/mol
$U_{xl,25\ °C} + 3/2O_{2g,25\ °C} = UO_{3xl,25\ °C}$	$\Delta H6 = \Delta H_f\ UO_3$ (*12*)
$2P_{xl,25\ °C} + 5/2O_{2g,25\ °C} = P_2O_{5xl,25\ °C}$	$\Delta H7 = \Delta H_f\ P_2O_5$ (*12*)
$H_{2g,25\ °C} + 1/2O_{2g,25\ °C} = H_2O_{l,25\ °C}$	$\Delta H8 = \Delta H_f\ H_2O$ (*12*)
$3U_{xl,25\ °C} + 2P_{xl,25\ °C} + 4H_{2g,25\ °C} + 9O_{2g,25\ °C} = (UO_2)_3(PO_4)_2 \cdot 4H_2O_{xl,25\ °C}$	$\Delta H12 = \Delta H_{f,el}(UP) = \Delta H11 + 3\Delta H6 + 2\Delta H7 + 4\Delta H8 = -7001.01 \pm 13.90$ kJ/mol

[a] Notes: xl = crystalline, sln = solution, *l* = liquid, *g* = gas, ox = oxide, el = element, ds = drop solution. [b] Two significant figures are reported to prevent rounding errors.

solutions that already contained stoichiometric concentrations of U, P, and Ca from additions of $UO_2(NO_3)_2$, $NH_4H_2PO_4$, and $Ca(NO_3)_2$, respectively, in the case of CaUP, to match the composition of the mineral phase of interest. An experiment was classified as supersaturated if at least one of the final concentrations of U, P, or Ca decreased from their starting values. The pH of each experimental solution was adjusted using minute quantities of concentrated HNO_3 and/or NaOH or KOH. The pH was monitored daily and adjusted as needed throughout each experiment. The pH descriptor for each experiment is the average of the pH values for the solubility plateau data points; however, the actual pH measurement for each data point was used in the subsequent thermodynamic calculations. Reaction vessels were sealed and agitated slowly end-over-end at room temperature. Aliquots of the experimental solution were extracted at various times, filtered through 0.1 μm Millipore Millex filters, diluted, and acidified for ICP-OES analysis to determine dissolved concentrations of U, P, and Ca with an analytical uncertainty of 3.5%. In these experiments the fraction able to pass through a 0.1 μm membrane is defined as dissolved and other methods of separation such as ultrafiltration may yield different results; however, the potential colloidal contribution to "solubility" is likely minimal due to the close correspondence of calculated log K_{sp} values from different pH conditions (see discussion below). Control experiments verified that loss of uranium through adsorption to the filter membrane and reaction vessel was negligible. To verify the composition of the mineral residue at the end of each experiment, ~10 mg of residue was collected for XRD analysis.

Calorimetry. Details of high temperature oxide melt solution calorimetry on uranyl-containing phases, design of the custom built Tian-Calvet twin calorimeter used in this study, and the standard calibration procedure against heat content of Al_2O_3 are previously described in detail (*4–9*). The samples were ground, pelletized, weighed using a semimicrobalance, and dropped from room temperature into the calorimeter with sodium molybdate ($3Na_2O-4MoO_3$) solvent at 702 °C. Constant bubbling with oxygen through the solvent (5 mL/min) was maintained to ensure oxidizing conditions and preserve U in the +6 oxidation state. Water was evolved into the gas space above the solvent and swept out of the calorimeter by O_2 flushing. Enthalpies of formation of HUP and UP from oxides and elements were calculated using thermodynamic cycles shown in Table 1, taking into account water content determined by TGA. Previously reported calorimetry results on UO_3 (*10*), P_2O_5 (*11*), and H_2O (*12*) were used as reference data.

Results and Discussion

High-Temperature Oxide-Melt Solution Calorimetry. Enthalpies of drop solution of $UO_2HPO_4 \cdot 3H_2O$ (HUP) and $(UO_2)_3(PO_4)_2 \cdot 4H_2O$ (UP) in sodium molybdate at 702 °C are 411.02 ± 3.46 kJ/mol and 821.38 ± 13.71 kJ/mol respectively (Table 1). The calculated enthalpies of formation from the binary oxides are (-240.95 ± 3.89) kJ/mol for HUP and (-681.51 ± 13.82) kJ/mol for UP. When normalized per one uranyl unit, this corresponds to (-240.95 ± 3.89) kJ/mol for HUP and (-227.17 ± 4.61) kJ/mol for the UP phase. These values indicate significant stability of both phases with respect to UO_3, P_2O_5 oxides, and H_2O. Note that we report enthalpies, free energies, and entropies to two decimal places, although the propagated errors do not justify that accuracy. This is done to avoid accumulated round-off errors in subsequent calculations.

HUP has a layered structure composed of uranyl phosphate layers with CaUP topology separated by hydrogen cations and water molecules (*13*). UP is a framework with uranyl phosphate layers (uranophane topology) joined by uranyl tetragonal bipyramids with water molecules located in the pores (*14*). Despite the structural dissimilarities shown, formation enthalpies indicate approximately equivalent stability of phases relative to constituent oxides. Thus, to identify the structural contribution or absence of such in phase stability, more uranyl phosphates of the analogous types should be studied.

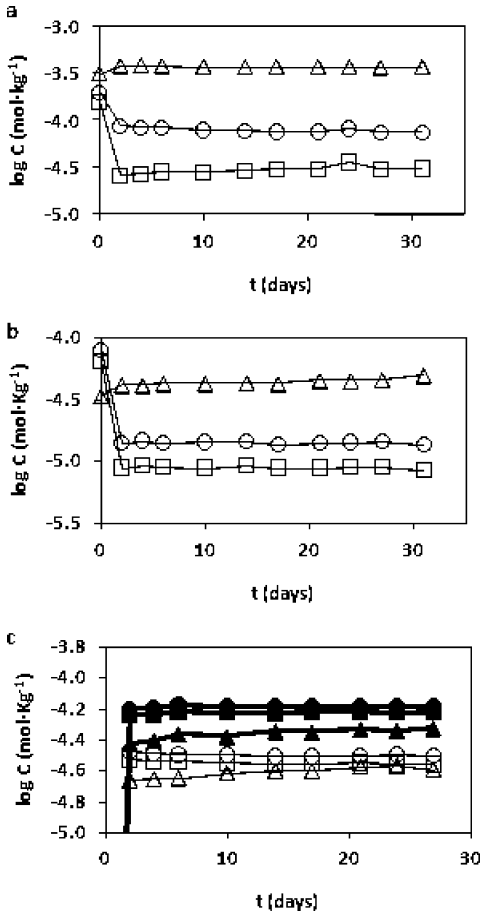

FIGURE 1. Plot of experimental measurements of the dissolved concentrations of U (squares), P (circles), and Ca (triangles) as log mol·kg^{-1} against time for CaUP from supersaturation for experiments at pH 3.0 (a) and pH 3.8 (b) and undersaturation for experiments at pH 3.5 (open symbols) and pH 3.1 (closed symbols) (c).

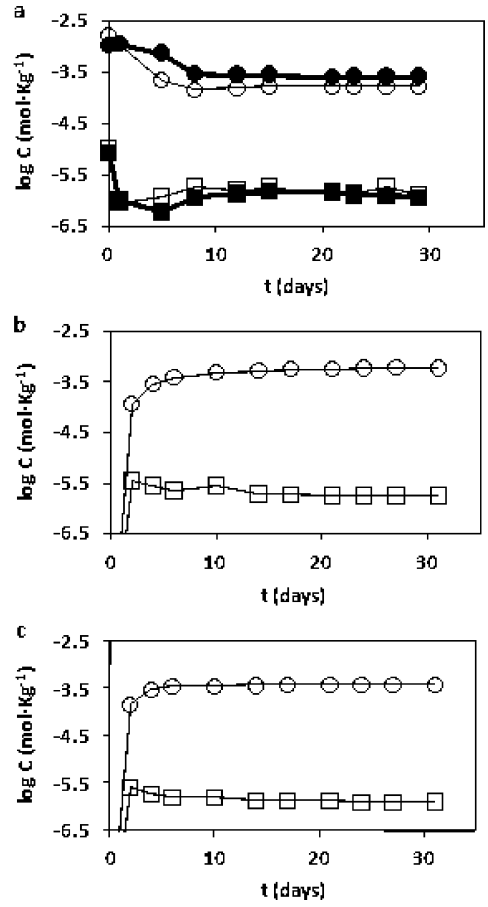

FIGURE 2. Plot of experimental measurements of the dissolved concentrations of U (squares) and P (circles) as log mol·kg^{-1} against time for HUP from supersaturation for experiments at pH 4.2 (open symbols) and pH 4.5 (closed symbols) (a) and undersaturation for experiments at pH 4.2 (b) and pH 4.5 (c).

The standard enthalpies of formation from the elements are (−3223.22 ± 3.99) kJ/mol for HUP and (−7001.01 ± 13.90) kJ/mol for UP.

Solubility Experiments. CaUP experiments involving supersaturated initial conditions at pH 3.0 and pH 3.8 reached a steady-state within 1 d (Figure 1a and b). Experiments from undersaturated conditions required additional time, 10 and 6 d, to attain a steady-state for experiments at pH 3.5 and 3.1, respectively (Figure 1c). All samples exhibited nonstoichiometric dissolution with higher Ca and P in solution than would be predicted based on congruent dissolution/precipitation of CaUP alone. Supersaturated experiments exhibited a greater extent of nonstoichiometric dissolution/precipitation than the under-saturated experiments. U:Ca and U:P molar ratios for supersaturated experiments were 0.2 and 0.4−0.6, respectively, while under-saturated experiments had U:Ca and U:P molar ratios of 1.2 and 0.9, respectively. XRD analysis of the mineral residues indicated that CaUP with decreased crystallinity was the only detectable mineral present, although the limitations of the XRD technique do not rule out the formation of a secondary phase that is either amorphous or in a small amount (less than ca. 5%) relative to the crystalline CaUP. Nonstoichiometric dissolution in these experiments could have been caused either by preferential leaching of Ca and P with incorporation of protons and/or water or by the formation of a uranyl phosphate secondary phase during the experiment. The former process would elevate the concentration of Ca and P relative to the stoichiometric concentration expected for U; the formation of a uranyl phosphate phase would depress the aqueous concentrations of U and P relative to the stoichiometric concentration expected for Ca. Our data cannot distinguish between these two possibilities and it is likely that both mechanisms may be taking place simultaneously. Preferential leaching of Ca may be partially driven by bond valence considerations (*13*). Reduced particle size as a result of preferential leaching can lead to artifacts in mineral residual XRD patterns consistent with decreased crystallinity such as broader peaks, a shift in peak locations, and extraneous peaks can appear. Preferential leaching of cations from uranyl minerals in aqueous solutions and decreased crystallinity in uranyl minerals resulting from leaching have been observed previously (*15, 16*). The formation of a leached layer or a secondary mineral phase during a solubility experiment does not nullify the results as long as there is still some contact and hence equilibration between the phase of interest and the bulk aqueous phase. The reversal measurements provide a test whether equilibrium was achieved, and K_{sp} values calculated from the undersaturation and supersaturation experiments should agree within experimental uncertainty if an equilibrium state was attained during the solubility experiments.

All the HUP experiments reached steady-state conditions within 10−12 d (Figure 2), and all experiments exhibited similar extents of nonstoichiometric dissolution, with P in excess of U in solution by more than 2 orders of magnitude. Analysis of mineral residues indicated that HUP was the only mineral present. Similar to the CaUP experiments, XRD analysis of the solids after the experimental runs indicated the presence only of HUP, although the degree of crystallinity

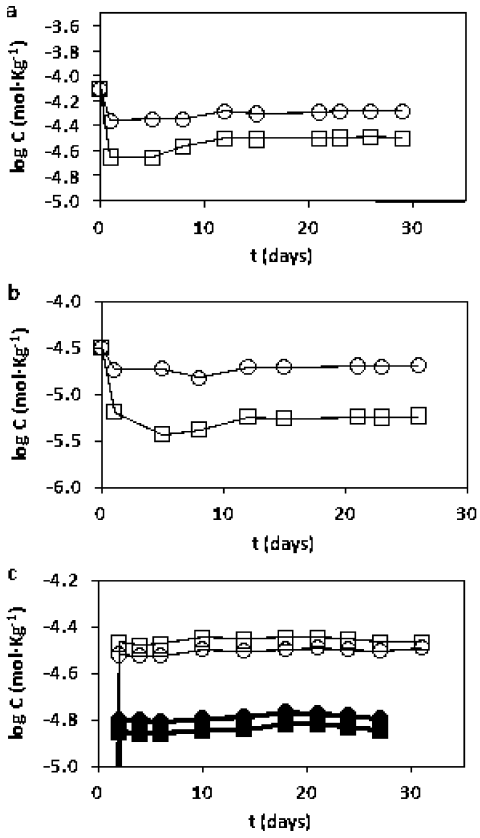

FIGURE 3. Plot of experimental measurements of the dissolved concentrations of U (squares) and P (circles) as log mol·kg^{-1} against time for UP from supersaturation for experiments at pH 3.1 (a) and pH 3.8 (b) and undersaturation for experiments at pH 3.1 (open symbols) and pH 3.5 (closed symbols) (c).

decreased during the equilibration time. Previous studies of uranyl mineral dissolution have also noted a decrease in crystallinity possibly with concurrent proton incorporation to maintain charge balance (*15, 16*). A similar mechanism could be occurring in this system with the leaching of P and possible incorporation of protons and other cation impurities as well as H_2O; however, the extent of preferential leaching was large and the difference in U and P concentrations may favor simultaneous leaching and secondary amorphous uranyl phase formation as an explanation.

UP experiments reached steady-state conditions within 10−12 d under all experimental conditions (Figure 3). Similar to the HUP experiments, all UP experiments exhibited nonstoichiometric dissolution with an excess of P in solution in three of the four conditions studied. The extent of excess P varied from one experiment to another. The pH 3.1 experiments that started from undersaturated conditions (Figure 3c) yielded an average U:P molar ratio of 1.1:1 which is close to the 1.5:1 molar ratio of stoichiometric dissolution, while all other experiments yielded average U:P molar ratios that ranged from 0.89:1 (Figure 3a) to 0.28:1 (Figure 3b). Final mineral residue analysis by XRD exhibited only peaks that can be attributed to UP; however, it is possible that a small amount (less than ca. 5%) of non-UP crystalline or amorphous precipitate was present. Similar to the other experiments in this study, the final residue showed a decreased extent of crystallinity relative to the starting material.

The preferential leaching of Ca and P in these experiments may suggest a steady state in the solid between the outer leached layer of the mineral and the bulk material. Our solubility results depict steady states between the aqueous solution and the outer leach layer of the minerals. A steady state between the aqueous solution and the inner bulk material may be implied if a steady state between the outer leach layer and the inner bulk material is indeed achieved. The similarity of solubility product values (see discussion below) for these systems that displayed different extents of leaching provides some support for this interpretation.

Solubility Product Calculations. Table 2 shows the reaction stoichiometry that we used for each mineral in the solubility product calculations. Solubility product (K_{sp}) calculations were only performed using data points that correspond to samples taken from each system after it had achieved steady-state conditions. The measured U, P, and Ca concentrations and corresponding measured pH values for each plateau data point that we used for the calculations are compiled in the Supporting Information Tables S2−S4. Ionic strength calculations for each plateau data point accounted for the concentrations of U, P, and Ca in the case of CaUP, the pH of each sample, and the known amount of NO_3^-, Na^+, and K^+ added from acid/base additions for pH adjustments. We used the extended Debye−Hückel equation to calculate the activity coefficients, γ_i, for each experimental condition:

$$\log \gamma_i = \frac{-Az_i^2\sqrt{I}}{1 + aB\sqrt{I}} + bI \qquad (1)$$

where I and z_i represent the ionic strength and ionic charge, respectively; A and B are constants with values of 0.51 and 0.32 (*17*), respectively, and a and b are values for a $RbNO_3$ electrolyte from Helgeson et al. (*17*), with values of 5.22 and 0.062, respectively. Parameters a and b take unique values for a particular electrolyte. To simplify the experimental systems, we did not buffer ionic strength with an added electrolyte. Because values of a and b have not been determined for uranyl-dominated systems, $RbNO_3$ was chosen as the most reasonable approximation for these experimental solutions, based on cation size, of those for which extended Debye−Hückel parameters are calculated (*17*).

Standard states employed in this study for solid phases and for H_2O are the pure mineral or fluid, respectively, at the temperature and pressure of the experiments. The standard state for aqueous species is defined as a hypothetical one molal solution whose behavior is that of infinite H_2O dilution at the temperature and pressure of interest. Molal activity coefficients of neutral aqueous species are assumed to be unity. Solubility product calculations for each plateau data point account for the aqueous complexation reactions listed in Supporting Information Table S5 to calculate UO_2^{+2}, PO_4^{-3}, and Ca^{2+} activities under each experimental condition from our measurements of total U, P, and Ca concentrations. Uncertainties associated with the stability constants in Table S5 (errors not shown) were not propagated through the K_{sp} calculations; however, the uncertainty in the experimental measurements likely dominates the errors associated with the K_{sp} values. Uncertainties associated with the aqueous stability constants in Table S5 would likely have a negligible effect on calculated K_{sp} values.

Calculated solubility products, averaged for all of the equilibrium measurements, with their 2σ uncertainties for each phase are listed in Table 2. In all cases, the solubility product values determined from experiments in which equilibrium was approached from undersaturation are within experimental uncertainty of the values determined from supersaturation experiments involving the same mineral phase. In addition, experiments conducted at different pH values using the same mineral phase yield solubility product values that are within experimental uncertainty of each other. The close correspondence between solubility product values from under- and supersaturated experiments, and from experiments conducted at different pH values suggests that

TABLE 2. Reaction Stoichiometry

mineral phase	dissolution reactions	mass action equations	log K_{sp} ± 2σ(I = 0)
autunite	$Ca(UO_2)_2(PO_4)_2 \cdot 3H_2O = Ca^{2+} + 2UO_2^{2+} + 2PO_4^{3-} + 3H_2O$	$K_{sp} = a_{Ca^{2+}} \cdot a^2_{UO_2^{2+}} \cdot a^2_{PO_4^{3-}}$	−48.36 (−0.03/+0.03)
uranyl hydrogen phosphate	$UO_2HPO_4 \cdot 3H_2O = UO_2^{2+} + HPO_4^{2-} + 3H_2O$	$K_{sp} = a_{UO_2^{2+}} \cdot a_{HPO_4^{2-}}$	−13.17 (−0.11/+0.07)
uranyl orthophosphate	$(UO_2)_3(PO_4)_2 \cdot 4H_2O = 3UO_2^{2+} + 2PO_4^{3-} + 4H_2O$	$K_{sp} = a^3_{UO_2^{2+}} \cdot a^2_{PO_4^{3-}}$	−49.36 (−0.04/+0.02)

	Gibbs free energy of formation equations	($\Delta G_f^\circ \pm 2\sigma$) (kJ mol^{-1})	($\Delta H_f^\circ \pm 2\sigma$) (kJ mol^{-1})	($\Delta S_f^\circ \pm 2\sigma$) (J mol^{-1}K^{-1})
autunite	$\Delta G_f^\circ = 3 \cdot \Delta G^\circ_{f(H_2O)} + \Delta G^\circ_{f(Ca^{2+})} + 2 \cdot \Delta G^\circ_{f(UO_2^{2+})} + 2 \cdot \Delta G^\circ_{f(PO_4^{3-})} - \Delta G_r^\circ$	−5496.35 (±9.67)		
uranyl hydrogen phosphate	$\Delta G_f^\circ = 3 \cdot \Delta G^\circ_{f(H_2O)} + \Delta G^\circ_{f(UO_2^{2+})} + \Delta G^\circ_{f(HPO_4^{2-})} - \Delta G_r^\circ$	−2835.14 (±4.89)	−3223.22 (±3.99)	−1302.28 (±21.18)
uranyl orthophosphate	$\Delta G_f^\circ = 4 \cdot \Delta G^\circ_{f(H_2O)} + 3 \cdot \Delta G^\circ_{f(UO_2^{2+})} + 2 \cdot \Delta G^\circ_{f(PO_4^{3-})} - \Delta G_r^\circ$	−6138.94 (±12.11)	−7001.01 (±13.90)	−2892.85 (±61.86)

the dissolution reactions listed in Table 2 correctly describe mineral dissolution in these systems. In addition, the close correspondence of the solubility product values from all experiments involving a particular mineral phase strongly suggests that these phases were stable under the experimental conditions and that the phases acted to buffer the U, P, and Ca concentrations in the experimental solutions.

Malgalhaes et al. (*18*) previously measured the solubility of synthetic CaUP that yielded a log K_{sp} value of −51.4 ± 0.11; however, the authors only made measurements from undersaturation and did not mention any postexperiment analysis of mineral residues. Guillaumont et al. (*19*) reviewed a solubility study of natural CaUP from undersaturation (*20*) and did not include the log K_{sp} value of −50.8 in their critical review because the composition of the mineral was not well established and the K_{sp} calculations failed to account for the formation of all aqueous uranyl phosphate complexes. In contrast, our study used a well-characterized natural mineral phase; we obtained steady-state data from supersaturated and undersaturated conditions; and our calculations included up-to-date stability constant values for aqueous complexes, yielding a more rigorously determined log K_{sp} value of −48.36 with 2σ uncertainty values of ±0.03.

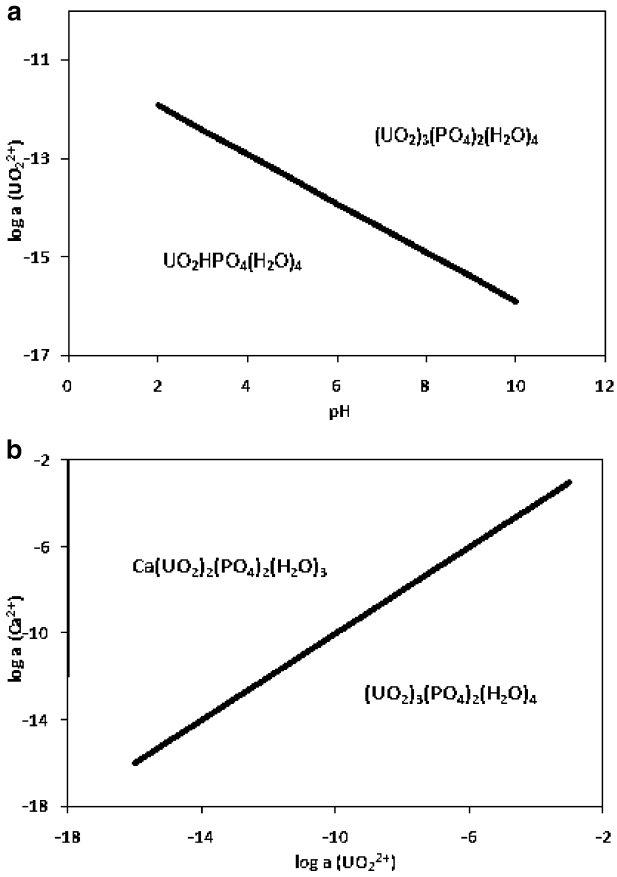

FIGURE 4. (a) Plot of the log of the aqueous uranyl cation activity as a function of pH, with the stability fields for UP and HUP, and the equilibrium line for reaction 4 depicted. The phase diagram is constructed for a PO_4^{-3} activity of 0.01 *m*. (b) Plot of the log of the aqueous Ca^{2+} activity as a function of the log of the aqueous uranyl cation activity, with the stability fields for UP and CaUP and the equilibrium line for reaction 6 depicted.

Previous measurements of HUP by Vesely et al. (*21*) and Van Haverbeke et al. (*22*) produced conditional log K_{sp} values (not extrapolated to infinite dilution) of −12.17 ± 0.07 and −10.38 ± 0.24, respectively. Markovic and Pavkovic (*23*) also performed solubility measurements on HUP and calculated an average log K_{sp} value of −12.33 ± 0.06. None of the previous studies rigorously demonstrated an equilibrium state by having the experimental systems approach equilibrium from both supersaturation and undersaturation. Postexperimental characterization by Markovic and Pavkovic (*23*) was extensive. Similarly, Van Haverbeke et al. (*22*) used XRD analysis to verify the identity of the mineral residues in their experiments, but Vesely et al. (*21*) did not report pre- or postexperimental XRD analysis. Our log K_{sp} value with its 2σ uncertainty, −13.17 (−0.11/+0.07) is outside the range of the previously reported values; however, it represents a value that has been extrapolated to the infinite dilution standard state, and it is based upon solubility data from systems in which equilibrium was approached from both supersaturation and undersaturation.

Previously reported values for the log K_{sp} of UP range from −49.00 to −53.33 (*21, 23–25*). Sandino et al. (*24*) and Rai et al. (*25*) performed extensive pre- and postexperimental characterization of the mineral phase. Van Haverbeke et al. (*22*) used XRD analysis to verify the identity of the mineral residues in their experiments, while Vesely et al. (*21*) did not mention pre- or postexperimental XRD analysis. All investigators gathered their data from undersaturated conditions with the exception of Sandino et al. (*24*) who did conduct both supersaturation and undersaturation experiments. Sandino et al. (*24*) and Rai et al. (*25*) both gathered data over a wide pH range (~3 to ~9); however, the calculated log K_{sp} values from their studies (−53.32 ± 0.17 and −49.08 ± 0.48, respectively) are not consistent. Our log K_{sp} value of −49.36 (−0.04/+ 0.02) is consistent with the log K_{sp} value calculated by Rai et al. (*25*).

Gibbs Free Energy of Formation. The calculated K_{sp} value for each solid phase can be used to calculate the standard

state Gibbs free energy of formation of the phase by first translating each K_{sp} value into a standard state Gibbs free energy of reaction, ΔG_r^o, for each dissolution reaction of interest using the following equation:

$$\Delta G_r^o = -2.3026RT \cdot \log K_{sp} \quad (2)$$

where R is the universal gas constant and T is absolute temperature. From the calculated values of ΔG_r^o, we used known standard state Gibbs free energies of formation of other components in the dissolution reactions (Table 2) to calculate the standard state Gibbs free energies of formation of the three solid phases studied here. Values obtained from Cox et al. (*26*) for $\Delta G_{f(UO_2^{2+})}^o$, $\Delta G_{f(PO_4^{3-})}^o$, $\Delta G_{f(HPO_4^{2-})}^o$, $\Delta G_{f(Ca^{2+})}^o$, and $\Delta G_{f(H_2O)}^o$ are -952.55 ± 1.75, -1025.49 ± 1.58, -1095.99 ± 1.58, -552.81 ± 1.05, and -237.14 ± 0.04 kJ/mol, respectively. To obtain the 2σ errors associated with the ΔG_r^o values, we propagated the largest error associated with the respective log K_{sp} values. Each data point from a solubility measurement yields calculated values for the Gibbs free energy of formation for the mineral of interest, and the average value for each mineral, with its 2σ error, is reported in Table 2. The 2σ errors are calculated from propagating the errors associated with the ΔG_f^o values of the mineral phase constituents and ΔG_r^o.

Chen et al. (*27*) predicted the Gibbs free energies of formation of various uranyl minerals using an empirical approach that derives the molar contributions of the structural components to ΔG_f^o and ΔH_f^o from thermodynamic data of phases for which the crystal structures are known. Model derived values for HUP and UP are -3063.5 and -6093.4 kJ/mol, respectively. Our values for HUP -2835.14 (± 4.89) kJ/mol and UP -6138.95 (± 12.11) kJ/mol are not consistent with those of Chen et al.; however, the HUP values are substantially closer to each other than the UP values. The better performance of the model for HUP is likely due to the use by Chen et al. (*26*) of previous HUP solubility measurements to develop the database for their model. Conversely, their prediction of the standard state Gibbs free energy of formation of UP was a "blind test" in that no previous UP data were used in the creation of the database for the prediction. These comparisons suggest that the accuracy of model derived thermodynamic properties of uranyl phases improves when the models can be based on experimental measurements involving the phase in question or a phase with structural components similar to the phase of interest.

Entropy of Formation and Standard Entropy. The entropy of formation from the elements ($\Delta S_{f,el}^o$) is calculated from Gibbs free energy of formation from the elements ($\Delta G_{f,el}^o$) determined from solubility measurements and enthalpy of formation ($\Delta H_{f,el}^o$) as measured by calorimetry:

$$\Delta G_{f,el}^o = \Delta H_{f,el}^o - T\Delta S_{f,el}^o \quad (3)$$

The calculated entropy of formation $\Delta S_{f,el}^o$ is -1302.28 (± 21.18) J/mol·K for HUP and -2892.85 (± 61.86) J/mol·K for UP. The standard entropy $S_{[]}^o$ thus could be determined from these values as -2774.13 (± 21.18) J/mol·K and -5494.70 (± 61.87) J/mol·K for HUP and UP, respectively.

Geologic Applications. The thermodynamic properties that have been determined in this study for CaUP, HUP, and UP can be used to determine the concentrations of aqueous species that control the relative stabilities of these phases. For example, the relationship between HUP and UP can be expressed:

$$H^+ + (UO_2)_3(PO_4)_2 \cdot 4H_2O \leftrightarrow UO_2HPO_4 \cdot 3H_2O + 2UO_2^{2+} + PO_4^{3-} + H_2O \quad (4)$$

Using standard Gibbs free energies of formation for the components in reaction 4 from Cox et al. (*26*) and from the results of this study yields a value for the ΔG_r^o of 136.09 kJ/mol and a log K value of -23.84. These values can be used to determine the relative stabilities of these phases as a function of pH and uranyl and phosphate activities in solution. At a PO_4^{3-} activity of 0.01 m, the equilibrium relationship (depicted in Figure 4a) can be expressed as:

$$\log \alpha_{UO_2^{2+}} = -0.5\ \mathrm{pH} - 10.92 \quad (5)$$

where $\log a_{UO_2^{2+}}$ represents the log of the activity of the uranyl cation in solution. Under low pH conditions, where the total aqueous uranium activity is virtually identical to the activity of the uranyl cation, eq 4 indicates that UP is more stable than HUP in uranium-contaminated waters. For example, at pH 4, when log $a_{UO_2^{2+}}$ (equivalent to the total aqueous uranium activity under low pH conditions) is greater than approximately -13, UP is the more stable phase. However, with increasing pH above 5, the activity of the uranyl cation decreases markedly due to the increased importance of uranyl aqueous complexes with hydroxide, carbonate, organic ligands, etc. Under these conditions, HUP can be the more stable phase, depending on the exact solution composition of interest.

The conditions that favor the formation of CaUP relative to UP are depicted in Figure 4b, which shows the equilibrium relationship:

$$UO_2^{2+} + H_2O + Ca(UO_2)_2(PO_4)_2 \cdot 3H_2O \leftrightarrow (UO_2)_3(PO_4)_2 \cdot 4H_2O + C_a^{2+} \quad (6)$$

The value of ΔG_r^o for reaction 6, based on standard state Gibbs free energies of formation from this study and from Cox et al. (*26*), is -5.72 kJ/mol, corresponding to a log K value of 1.00. As the position of the equilibrium line in Figure 4b indicates, CaUP is more stable than UP whenever the activity of Ca^{2+} is more than an order of magnitude larger than the activity of UO_2^{2+}. For contaminated geologic systems, this condition is likely met under a range of pH conditions, and UP would be more stable than CaUP only in Ca-poor waters that are highly contaminated with uranium.

Acknowledgments

Funding for this research was provided in part by a U.S. Department of Energy, Office of Science and Technology and International (OST&I) grant under the Source Term Thrust program, and in part by a U.S. Department of Energy, Environmental Remediation Science Program grant. Calorimetry measurements were supported by the U.S. Department of Energy (grant DE-FG02-97ER14749).

Supporting Information Available

Details of the syntheses, mineral characterization, and data points used for calculating thermodynamic parameters. This material is available free of charge via the Internet at http://pubs.acs.org.

Literature Cited

(1) Wellman, D. M.; Gunderson, K. M.; Icenhower, J. P.; Forrester, S. W. Dissolution kinetics of synthetic and natural meta-autunite minerals, X-3-n((n)+) $[(UO_2)(PO_4)]_2 \cdot xH_2O$, under acidic conditions. *Geochem. Geophys. Geosyst.* **2007**, *8*, 1–16.

(2) Gorman-Lewis, D.; Burns, P. C.; Fein, J. B. Review of Uranyl Mineral Solubility Measurements. *J. Chem. Thermodyn.* **2008**, *40*, 335–352.

(3) Illingworth, J. A. A Common Source of Error in pH Measurements. *Biochem. J.* **1981**, *195* (1), 259–262.

(4) Gorman-Lewis, D. J.; Mazeina, L.; Fein, J. B.; Szymanowski, J.; Burns, P. C.; Navrotsky, A. Thermodynamic properties of soddyite from solubility and calorimetric measurements. *J. Chem. Thermodyn.* **2007**, *39* (4), 568–575.

(5) Kubatko, K.-A.; Helean, K.; Navrotsky, A.; Burns, P. C. Thermodynamics of uranyl minerals: enthalpies of formation of uranyl oxide hydrates. *Am. Mineral.* **2006**, *91* (4), 658–666.

(6) Kubatko, K. A.; Helean, K. B.; Navrotsky, A.; Burns, P. C. Thermodynamics of uranyl minerals: Enthalpies of formation of rutherfordine, UO_2CO_3, andersonite, $Na_2CaUO_2(CO_3)_3(H_2O)_5$, and grimselite, $K_3NaUO_2(CO_3)_3H_2O$. *Am. Mineral.* **2005**, *90* (8−9), 1284–1290.

(7) Kubatko, K. A. H.; Helean, K. B.; Navrotsky, A.; Burns, P. C. Stability of peroxide-containing uranyl minerals. *Science* **2003**, *302* (5648), 1191–1193.

(8) Navrotsky, A. Progress and New Directions in High-Temperature Calorimetry. *Phys. Chem. Miner.* **1977**, *2* (1−2), 89–104.

(9) Navrotsky, A. Progress and new directions in high temperature calorimetry revisited. *Phys. Chem. Miner.* **1997**, *24* (3), 222–241.

(10) Helean, K. B.; Navrotsky, A.; Vance, E. R.; Carter, M. L.; Ebbinghaus, B.; Krikorian, O.; Lian, J.; Wang, L. M.; Catalano, J. G. Enthalpies of formation of Ce-pyrochlore, $Ca_{0.93}Ce_{1.00}Ti_{2.035}O_{7.00}$, U-pyrochlore, $Ca_{1.46}U_{0.234} + U_{0.466} + Ti_{1.85}O_{7.00}$ and Gd-pyrochlore, $Gd_2Ti_2O_7$: three materials relevant to the proposed waste form for excess weapons plutonium. *J. Nucl. Mater.* **2002**, *303* (2−3), 226–239.

(11) Ushakov, S. V.; Helean, K. B.; Navrotsky, A.; Boatner, L. A. Thermochemistry of rare-earth orthophosphates. *J. Mater. Res.* **2001**, *16* (9), 2623–2633.

(12) Robie, R. A.; Hemingway, B. S. Thermodynamic properties of minerals and related substances at 298.15K and 1 bar (105 pascals) and at higher temperatures. *U.S. Geological Survey Bulletin* **1995**, 2131.

(13) Burns, P. C. The Crystal Chemistry of Uranium. In *Uranium: Mineralogy, Geochemistry and the Environment*; Burns, P. C., Finch, R. J., Eds.; Mineralogical Society of America: Washington DC, 1999; Vol. 38, pp 23−90.

(14) Locock, A. J.; Burns, P. C. The crystal structure of triuranyl diphosphate tetrahydrate. *J. Solid State Chem.* **2002**, *163* (1), 275–280.

(15) Gorman-Lewis, D.; Fein, J. B.; Burns, P. C.; Szymanowski, J. E. S.; Converse, J. Solubility measurements of the uranyl oxide hydrate phases metaschoepite, compreignacite, Na-compreignacite, becquerelite, and clarkeite. *J. Chem. Thermodyn.* **2008**, *40* (6), 980–990.

(16) Schindler, M.; Hawthorne, F. C.; Burns, P. C.; Maurice, P. A. Dissolution of uranyl-oxide-hydroxy-hydrate minerals. II. Becquerelite. *Can. Mineral.* **2006**, *44*, 1207–1225.

(17) Helgeson, H. C.; Kirkham, D. H.; Flowers, G. C. Theoretical Prediction of the Thermodynamic Behavior of Aqueous-Electrolytes at High-Pressures and Temperatures: IV. Calculation of Activity-Coefficients, Osmotic Coefficients, and Apparent Molal and Standard and Relative Partial Molal Properties to 600 °C and 5 KB. *Am. J. Sci.* **1981**, *281* (10), 1249–1516.

(18) Magalhaes, M. C. F.; Pedrosa de Jesus, J. D.; Williams, P. A. The chemistry of uranium dispersion in groundwaters at the Pinhal do Souto mine, Portugal. *Inorg. Chim. Acta* **1985**, *109* (2), 71–8.

(19) Guillaumont, R.; Fanghanel, T.; Fuger, J.; Grenthe, I.; Neck, V.; Palmer, D.; Rand, M. *Update on the Chemical Thermodynamics of Uranium, Neptunium, and Plutonium,* 2nd ed.; Elsevier: Amsterdam, 2003; p 919.

(20) Muto, T. Thermochemical stability of ningyoite. *Mineral. J.* **1965**, *4*, 245–274.

(21) Vesely, V.; Pekarek, V.; Abbrent, M. A study of uranyl phosphates III: Solubility products of uranyl hydrogen phosphate, uranyl orthophosphate and some alkali uranyl phosphates. *J. Inorg. Nucl. Chem.* **1965**, *27*, 1159–1166.

(22) VanHaverbeke, L.; Vochten, R.; VanSpringel, K. Solubility and spectrochemical characteristics of synthetic chernikovite and meta-ankoleite. *Mineral. Mag.* **1996**, *60* (402), 759–766.

(23) Markovic, M.; Pavkovic, N. Solubility and Equilibrium-Constants of Uranyl(2+) in Phosphate Solutions. *Inorg. Chem.* **1983**, *22* (6), 978–982.

(24) Sandino, A.; Bruno, J. The Solubility of $(UO_2)_3(PO_4)_2(H_2O)_{4(S)}$ and the Formation of U(VI) Phosphate Complexes - Their Influence in Uranium Speciation in Natural-Waters. *Geochim. Cosmochim. Acta* **1992**, *56* (12), 4135–4145.

(25) Rai, D.; Xia, Y. X.; Rao, L. F.; Hess, N. J.; Felmy, A. R.; Moore, D. A.; McCready, D. E. Solubility of $(UO_2)_3(PO_4)_2 \cdot 4H_2O$ in H^+-Na^+-OH^--H_2PO_4-HPO_4^{2-}-PO_4^{3-}-H_2O and its comparison to the analogous PuO_2^{2+} system. *J. Solution Chem.* **2005**, *34* (4), 469–498.

(26) Cox, J. D.; Wagman, D. D.; Medvedev, V. A. *CODATA Key Values for Thermodynamics*; Hemisphere Publishing Corporation: New York, 1989.

(27) Chen, F. R.; Ewing, R. C.; Clark, S. B. The Gibbs free energies and enthalpies of formation of U^{6+} phases: An empirical method of prediction. *Am. Mineral.* **1999**, *84* (4), 650–664.

ES9012933